Original article

Error Growth in Three-Dimensional Homogeneous Turbulence

Katsunori Yoshimatsu[1] and Taketo Ariki[2]

[1] Institute of Materials and Systems for Sustainability, Nagoya University, Nagoya, 464-8601, Japan
[2] Department of Aerospace Engineering, Tohoku University, Sendai 980-8597, Japan

Email: yoshimatsu@nagoya-u.jp

J. Phys. Soc. Jpn. **88**, 124401 (2019).
DOI: 10.7566/JPSJ.88.124401
(Received June 22, 2019; accepted October 7, 2019; published online November 8, 2019)

Error Growth in Three-Dimensional Homogeneous Turbulence

Katsunori Yoshimatsu[1 *] and Taketo Ariki[2]

[1] *Institute of Materials and Systems for Sustainability, Nagoya University, Nagoya, 464-8601, Japan*

[2] *Department of Aerospace Engineering, Tohoku University, Sendai 980-8597, Japan*

We study the evolution of an error field defined by the difference between two velocity fields in statistically identical three-dimensional incompressible homogeneous turbulence. We assume that the initial error resides only in a high wavenumber range. A theoretical analysis based on a self-similarity assumption for the large-scale error field evolution shows that the growth of the error energy spectrum is characterized by both the total error energy and the integral length scales of the error field. Direct numerical simulation (DNS) of the error field in incompressible turbulence in a periodic box shows that this characterization holds well in a time period. In addition, scale-dependent error energy production is discussed by using the DNS.

1. Introduction

Turbulence has strong nonlinearity and a large number of eddies exhibiting a wide range of dynamically active scales. The time histories of flow quantities such as the velocity at any fixed position are chaotic and therefore unpredictable, while the evolution of turbulent statistics, e.g., the total kinetic energy and the total enstrophy, are reproducible. Let us consider two statistically identical turbulent flows whose initial conditions are slightly different from each other but whose boundary conditions are identical. The error field is defined by the difference between the two velocity fields of the flows. Since the pioneering work by Lorenz,[1)] many studies have been conducted on the growth of the error field (e.g., see Refs. 2 and 3). The correlation length scale of the error field increases as time progresses. At each wavenumber, the error energy spectrum grows with time and saturates when the scale-by-scale correlation between the velocity fields is completely lost.

We here confine ourselves to error growth in three-dimensional (3D) incompressible homogeneous turbulence, which is one of the most canonical turbulent flows. The first obser-

*yoshimatsu@nagoya-u.jp

vation of error growth using direct numerical simulation (DNS) was provided for 3D freely decaying turbulence in a periodic box.[4] Using the test-field model, an Eulerian closure theory, of the isotropic turbulence, Leith and Kraichnan[5] showed error energy amplification and backward error energy transfer. In addition, they found an error energy spectrum $E_\delta(k,t)$ obeying the form that $E_\delta(k,t) = \Lambda(t)k^4 + o(k^4)$ at small k in an infinitely wide inertial subrange of the isotropic turbulence, where k is the wavenumber and $\Lambda(t)$ is a function of only the time t. This k^4 form was shown for isotropic turbulence at sufficiently high Reynolds number by numerical calculation based on an eddy-damped quasi-normal Markovian (EDQNM) model.[6] It was suggested that this form arises from the large-scale property of $E_\delta(k)$ at $k \to 0$.[2,6] The EDQNM results were verified by large-eddy simulation.[7] The predictability was also characterized by the Lyapunov exponents of the error field.[8–11]

The large-scale structure of a velocity field, which can be characterized by the velocity correlation spectral tensor at $k \to 0$, in 3D incompressible homogeneous turbulence plays significant roles in the decay of the turbulence even though the Reynolds number is not high enough.[12–15] In this paper, we study the contributions of the error field at large scales including the scales of the error energy containing range on the error growth for two statistically identical velocity fields in 3D incompressible homogeneous turbulence. An identical external force is imposed on the velocity fields. In Sec. 2, we theoretically analyze the large-scale structure of the error field, and discuss the implications of a self-similarity assumption of the error growth at the large scales. We focus on the case where the scales of the error energy containing range are much smaller than the integral length scales of the velocity fields. In Sec. 3, we examine whether the theoretical results hold well for DNS of two nearly statistically identical velocity fields in incompressible turbulence in a periodic box. Moreover, the scale-dependent nonlinear interactions are studied by using the DNS. Finally, Sec. 4 provides our conclusions.

2. Basic Equations and Statistics of an Error Field

2.1 Basic equations

We consider two 3D incompressible homogeneous turbulent flows subject to an identical external forcing $\boldsymbol{F}(\boldsymbol{x},t)$, where $\boldsymbol{x}$ is the position in the Cartesian coordinate system and $\boldsymbol{x} = (x_1, x_2, x_3)$. We assume that their initial fields are slightly different from each other. Their velocity fields, denoted by $\boldsymbol{u}^{(0)}(\boldsymbol{x},t)$ and $\boldsymbol{u}^{(1)}(\boldsymbol{x},t)$, obey the Navier-Stokes equations,

$$\partial_t \boldsymbol{u}^{(s)} + (\boldsymbol{u}^{(s)}\cdot\nabla)\boldsymbol{u}^{(s)} = -\frac{1}{\rho}\nabla p^{(s)} + \nu\nabla^2\boldsymbol{u}^{(s)} + \boldsymbol{F}, \tag{1}$$

with $\nabla\cdot\boldsymbol{u}^{(s)} = 0$ ($s = 0, 1$), where $p^{(s)}(\boldsymbol{x}, t)$ is the pressure, ν is the kinematic viscosity, ρ is the fluid density, $\partial_t = \partial/\partial t$, $\nabla = (\partial_1, \partial_2, \partial_3)$, and $\partial_j = \partial/\partial x_j$. We omit the arguments $\boldsymbol{x}$ and t and write $\boldsymbol{u}^{(0)}$ as $\boldsymbol{u}$ for brevity, unless otherwise stated. We set $\langle \boldsymbol{u}^{(s)}\rangle = \boldsymbol{0}$, where $\langle\cdot\rangle$ denotes an ensemble average of $\cdot$. In homogeneous turbulence, $\langle\cdot\rangle$ is independent of the position $\boldsymbol{x}$ and can be regarded as the spatial average.

The error field $\boldsymbol{\xi}(\boldsymbol{x}, t)$ is defined as $\boldsymbol{\xi} = \boldsymbol{u}^{(1)} - \boldsymbol{u}$. Equation (1) gives

$$\partial_t\boldsymbol{\xi} = -(\boldsymbol{\xi}\cdot\nabla)\boldsymbol{u} - \{(\boldsymbol{\xi} + \boldsymbol{u})\cdot\nabla\}\boldsymbol{\xi} - \frac{1}{\rho}\nabla\left(p^{(1)} - p^{(0)}\right) + \nu\nabla^2\boldsymbol{\xi}, \tag{2}$$

with $\nabla\cdot\boldsymbol{\xi} = 0$. Equation (2) yields

$$\frac{1}{2}\partial_t\langle|\boldsymbol{\xi}|^2\rangle = \langle(\partial_j\xi_i)\xi_j u_i\rangle - \nu\langle\partial_j\xi_i\partial_j\xi_i\rangle, \tag{3}$$

where the summation convention is used for repeated alphabetical subscripts. The total error energy $(1/2)\langle|\boldsymbol{\xi}|^2\rangle$ is not conservative for inviscid flow, because $\langle(\partial_j\xi_i)\xi_j u_i\rangle$ on the right-hand side of Eq. (3) can produce the error energy.

In the homogeneous turbulence, we define the velocity correlation spectral tensor $\hat{R}^{(s)}_{ij}(\boldsymbol{k}, t)$ ($s = 0, 1$) and the error field correlation spectral tensor $\hat{D}_{ij}(\boldsymbol{k}, t)$ as the Fourier transform of the two-point velocity correlation $R^{(s)}_{ij}(\boldsymbol{r}, t)$ and the two-point correlation of the error field $D_{ij}(\boldsymbol{r}, t)$, respectively, where $\boldsymbol{k}$ is the wave vector, $R^{(s)}_{ij}(\boldsymbol{r}) = \langle u^{(s)}_i(\boldsymbol{x})u^{(s)}_j(\boldsymbol{x} + \boldsymbol{r})\rangle$ and $D_{ij}(\boldsymbol{r}, t) = \langle\xi_i(\boldsymbol{x})\xi_j(\boldsymbol{x} + \boldsymbol{r})\rangle$. Here, $\hat{\cdot}$ denotes the Fourier transform of $\cdot$ such that $\hat{\psi}(\boldsymbol{k}, t) = (2\pi)^{-3}\int_{\mathbb{R}^3}\psi(\boldsymbol{r}, t)\exp(-i\boldsymbol{k}\cdot\boldsymbol{r})d\boldsymbol{r}$. We then define the kinetic energy spectra $E^{(s)}(k, t)$ and the error energy spectrum $E_\delta(k, t)$ as

$$E^{(s)}(k, t) = \frac{1}{2}\int \hat{R}^{(s)}_{ii}(\boldsymbol{q}, t)dS_k, \tag{4}$$

$$E_\delta(k, t) = \frac{1}{2}\int \hat{D}_{ii}(\boldsymbol{q}, t)dS_k, \tag{5}$$

where $k = |\boldsymbol{k}|$ and $\int\cdot dS_k$ denotes the integral of $\cdot$ over the spherical surface with a radius of $|\boldsymbol{q}| = k$ and a center at $\boldsymbol{q} = \boldsymbol{0}$. The integral length scale of $g(\boldsymbol{x}, t)$ in the jth Cartesian direction is defined as

$$L_j(g) = \frac{\int_0^\infty\langle g(\boldsymbol{x}, t)g(\boldsymbol{x} + r\boldsymbol{e}_j, t)\rangle dr}{\langle g^2(\boldsymbol{x}, t)\rangle}, \tag{6}$$

where $\boldsymbol{e}_j$ is the unit vector pointing to the jth direction, and $g = u_i$ or ξ_i.

2.2 *Large-scale structure of the error field*

We study here the large-scale structure of the error field in 3D incompressible homogeneous turbulence. The large-scale structure of the error field can be characterized by the error field correlation spectral tensor $\hat{D}_{ij}(\boldsymbol{k}, t)$. We assume that $\hat{D}_{ii}(\boldsymbol{k}, t)$ at an initial time instant $t = t_0$ is nonzero only in a sufficiently high wavenumber range. The velocity correlation spectral tensor $\hat{R}^{(0)}_{ij}(\boldsymbol{k}, t_0)$ is identical to $\hat{R}^{(1)}_{ij}(\boldsymbol{k}, t_0)$ in the $\boldsymbol{k}$ range where $\hat{D}_{ii}(\boldsymbol{k}, t_0) = 0$. The error energy spectrum $E_\delta(k, t)$ can grow with time t, until the correlation between $\hat{\boldsymbol{u}}^{(0)}(\boldsymbol{k}, t)$ and $\hat{\boldsymbol{u}}^{(1)}(\boldsymbol{k}, t)$ is completely lost at each k. In other words, the inequality, $E_\delta(k, t) \leq 2E^{(s)}(k, t)$, can hold for any k. Accordingly, it is natural to assume that $\hat{D}_{ij}(\boldsymbol{k}, t) = O(k^b)$ at $k \to 0$ if $\hat{R}^{(s)}_{ij}(\boldsymbol{k}, t) = O(k^c)$ at $k \to 0$, where $b \geq c$.

As is the case of so-called Batchelor turbulence[16,17] in which the velocity correlation spectral tensor at $\boldsymbol{k} \to \boldsymbol{0}$ is $O(k^2)$, we assume that

$$\hat{D}_{ij}(\boldsymbol{k}, t) = O(k^2) \tag{7}$$

at $\boldsymbol{k} \to \boldsymbol{0}$ and at a certain time instant $t = t_1 (> t_0)$. Equation (7) implies that $E_\delta(k, t)$ takes the form

$$E_\delta(k, t) = \Lambda(t)k^4 + o(k^4) \tag{8}$$

at $k \to 0$.

The tensor $\hat{D}_{ij}(\boldsymbol{k}, t)$ obeys the following equation derived from Eq. (2) with the divergence free conditions $\nabla\cdot\boldsymbol{u} = 0$ and $\nabla\cdot\boldsymbol{\xi} = 0$:

$$\begin{aligned} \partial_t \hat{D}_{ij}(\boldsymbol{k}, t) \quad = \quad & ik_l \Big[P_{im} \left\{ \hat{W}_{lmj}(\boldsymbol{k}) + \hat{W}_{mlj}(\boldsymbol{k}) + \hat{V}_{lmj}(\boldsymbol{k}) \right\} \\ & - P_{jm} \left\{ \hat{W}_{lmi}(-\boldsymbol{k}) + \hat{W}_{mli}(-\boldsymbol{k}) + \hat{V}_{mli}(-\boldsymbol{k}) \right\} \Big] - 2\nu k^2 \hat{D}_{ij}(\boldsymbol{k}, t), \end{aligned} \tag{9}$$

where $P_{ij} = \delta_{ij} - k_i k_j / k^2$, δ_{ij} is Kronecker's delta, and $\hat{V}_{ijl}(\boldsymbol{k})$ and $\hat{W}_{ijl}(\boldsymbol{k})$ are the Fourier transforms of $V_{ijl}(\boldsymbol{r})$ and $W_{ijl}(\boldsymbol{r})$, respectively, defined as

$$V_{ijl}(\boldsymbol{r}) \ = \ \langle \xi_i(\boldsymbol{x}) \xi_j(\boldsymbol{x}) \xi_l(\boldsymbol{x} + \boldsymbol{r}) \rangle, \tag{10}$$

$$W_{ijl}(\boldsymbol{r}) \ = \ \langle \xi_i(\boldsymbol{x}) u_j(\boldsymbol{x}) \xi_l(\boldsymbol{x} + \boldsymbol{r}) \rangle. \tag{11}$$

Furthermore, $k_l \hat{V}_{ijl}(\boldsymbol{k}) = k_l \hat{W}_{ijl}(\boldsymbol{k}) = 0$, because $(\partial/\partial r_l) V_{ijl}(\boldsymbol{r}) = 0$ and $(\partial/\partial r_l) W_{ijl}(\boldsymbol{r}) = 0$. Provided that $\hat{V}_{ijl}(\boldsymbol{k})$ and $\hat{W}_{ijl}(\boldsymbol{k})$ can be respectively rewritten as $\hat{V}_{ijl}(\boldsymbol{k}) = \hat{V}^0_{ijl} + O(k)$ and $\hat{W}_{ijl}(\boldsymbol{k}) = \hat{W}^0_{ijl} + O(k)$ at $\boldsymbol{k} \to \boldsymbol{0}$, then $k_l \hat{V}^0_{ijl} = k_l \hat{W}^0_{ijl} = 0$ for any $\boldsymbol{k}$. Therefore, $\hat{V}^0_{ijl} = 0$ and $\hat{W}^0_{ijl} = 0$. Accordingly, we find that at $\boldsymbol{k} \to \boldsymbol{0}$,

$$\partial_t \hat{D}_{ij}(\boldsymbol{k}, t) = O(k^2) \tag{12}$$

which implies that Eq. (7) holds for any $t\ (\geq t_1)$ and that the time derivative of Λ in Eq. (8) need not be zero in general for any $t\ (\geq t_1)$. The closure theories[5,6] showed that $\partial_t E_\delta(k, t) > 0$ in the inertial subrange for developed isotropic error fields in 3D incompressible isotropic turbulence.

Instead of Eq. (7), we can assume that, at an initial time instant $\tilde{t}_0$, $\hat{D}_{ij}(\boldsymbol{k}) = O(k^0)$, and therefore that $E_\delta(k, \tilde{t}_0) = \Lambda_2 k^2 + o(k^2)$, where Λ_2 is a k-independent constant. On the basis of the arguments of Refs. 14, 18, and 19 about the large-scale structure of velocity fields in incompressible homogeneous turbulence, it is shown that Λ_2 is time independent under an appropriate condition. This independence means that $\Lambda_2 = 0$ for any $t(\geq \tilde{t}_0)$, if we consider only the case in which the initial error energy spectrum is confined to a high enough wavenumber range.

2.3 *Self-similar evolution of the error field*

First, we introduce a vector potential $\boldsymbol{a}(\boldsymbol{x}, t)$ such that $\boldsymbol{\xi} = \nabla \times \boldsymbol{a}$ and $\nabla \cdot \boldsymbol{a} = 0$. The correlation spectral tensor $\hat{A}_{\alpha\alpha}(\boldsymbol{k}, t)$ is defined by the Fourier transform of $\langle a_\alpha(\boldsymbol{x}, t) a_\alpha(\boldsymbol{x}+\boldsymbol{r}, t)\rangle$, where we use no summation convention for the Greek subscripts. Equations (7) and (12) mean $\hat{A}_{\alpha\alpha}(\boldsymbol{k}, t) = O(k^0)$ and $\partial_t \hat{A}_{\alpha\alpha}(\boldsymbol{k}, t) = O(k^0)$, respectively. Therefore, because $\nabla \cdot \boldsymbol{a} = 0$, $\hat{A}_{\alpha\alpha}(\boldsymbol{k}, t)$ at $\boldsymbol{k} \to \boldsymbol{0}$ can be written as

$$\hat{A}_{\alpha\alpha}(\boldsymbol{k}, t) = P_{i\alpha} P_{j\alpha} M_{ij}(t) + o(1), \tag{13}$$

where $M_{ij}(t)$ is time dependent and $\boldsymbol{k}$ independent. In this paper, we consider a case in which the force $\boldsymbol{F}$ is identical so that no external force is imposed on the error field. Therefore, we assume that the time dependence of $M_{ij}(t)$ is independent of i and j for nonzero $M_{ij}(t)$ after a transient time period, and we set $M_{ij}(t) = C(t)\tilde{M}_{ij}$, where $\tilde{M}_{ij}$ is independent of time t. This time independence implies that $\hat{A}_{\alpha\alpha}(\boldsymbol{k}, t)/C(t)$ is time independent at $\boldsymbol{k} \to \boldsymbol{0}$ for any fixed $\boldsymbol{k}/k$.

Next, we argue a certain self-similarity of $\hat{A}_{\alpha\alpha}(\boldsymbol{k}, t)$, similar to the argument of Ref. 18 that discussed a type of self-similarity of the velocity correlation spectral tensor taking a form of $O(k^0)$ at $\boldsymbol{k} \to \boldsymbol{0}$. We assume that $\hat{A}_{\alpha\alpha}(\boldsymbol{k}, t)$ evolves at large scales including the scales comparable to the integral length scale of the error field in accordance with a self-similar form

$$\hat{A}_{\alpha\alpha}(\boldsymbol{k}, t) = C(t) f_{\alpha\alpha}(\boldsymbol{\zeta}), \tag{14}$$

in a certain time range and domain of the wave vector space $\boldsymbol{k}$ including small enough k range, where $\boldsymbol{\zeta}$ is a self-similar variable defined as $\boldsymbol{\zeta} = (k_1\ell_1(t), k_2\ell_2(t), k_3\ell_3(t))$, $f_{\alpha\alpha}(\boldsymbol{\zeta})$ is a dimensionless function, and $\ell_m(t)$ is a length scale in the mth Cartesian direction. Because $\hat{A}_{\alpha\alpha}(\boldsymbol{k}, t) = O(k^0)$ at $\boldsymbol{k} \to \boldsymbol{0}$, $f_{\alpha\alpha}(\boldsymbol{\zeta}) = O(|\boldsymbol{\zeta}|^0)$ at $\boldsymbol{\zeta} \to \boldsymbol{0}$. It should be noted that $C(t)$ has dimensions of (velocity)^2×(length)^5. We do not impose self-similarity in the viscosity-dominant wave vector range for the error field where the nonlinear error energy production is negligible compared to the error energy dissipation. The coefficient $C(t)$ in Eq. (14) arises from the time independence of $f_{\alpha\alpha}(\boldsymbol{\zeta})$ at $\boldsymbol{\zeta} \to \mathbf{0}$ for fixed $\boldsymbol{\zeta}/|\boldsymbol{\zeta}|$ and the time dependence of $\hat{A}_{\alpha\alpha}(\boldsymbol{k}, t)$ at $\boldsymbol{k} \to \mathbf{0}$ for fixed $\boldsymbol{k}/k$. Note that $\boldsymbol{\zeta}/|\boldsymbol{\zeta}|(= \boldsymbol{k}/k)$ is time independent for fixed $\boldsymbol{k}$, if $\boldsymbol{k}/k = (1, 0, 0)$, $(0, 1, 0)$ or $(0, 0, 1)$.

In the algebra similar to that used by Ref. 18, we find that

$$\ell_j/\ell_i \simeq \text{const.} \tag{15}$$

for any i and j in the self-similar evolution. The details of the algebra are shown in the Appendix. The length scale ℓ_m can be rewritten as $\ell_m = c_m\ell(t)$, where c_m is a constant. We assume that the time dependence of ℓ_m is independent of the component α. We can therefore set $\boldsymbol{\zeta} = \boldsymbol{k}\ell$ instead of $\boldsymbol{\zeta} = (k_1\ell_1(t), k_2\ell_2(t), k_3\ell_3(t))$. The spectral correlation tensor of the error field $\hat{D}_{\alpha\alpha}(\boldsymbol{k}, t)$ can be rewritten as

$$\hat{D}_{\alpha\alpha}(\boldsymbol{k}, t) = (k^2 - k_\alpha^2)\hat{A}_{ii}(\boldsymbol{k}, t) - k^2\hat{A}_{\alpha\alpha}(\boldsymbol{k}, t) = C(t)\ell^{-2}(t)h_{\alpha\alpha}(\boldsymbol{\zeta}), \tag{16}$$

at the large scales, where $h_{\alpha\alpha}(\boldsymbol{\zeta}) = (|\boldsymbol{\zeta}|^2 - \zeta_\alpha^2)f_{ii}(\boldsymbol{\zeta}) - |\boldsymbol{\zeta}|^2 f_{\alpha\alpha}$.

We assume that Eq. (16) is a good approximation of $\hat{D}_{\alpha\alpha}(\boldsymbol{k}, t)$ in the $(\boldsymbol{k}, t)$ range and that the right-hand side of Eq. (16) mostly contributes to integrals such as $\int_{\mathbb{R}^3} \hat{D}_{\alpha\alpha}(\boldsymbol{k}, t)d\boldsymbol{k}$. Substitution of Eq. (16) into $\int_{\mathbb{R}^3} \hat{D}_{\alpha\alpha}(\boldsymbol{k}, t)d\boldsymbol{k}$ shows that

$$\begin{aligned} \langle\xi_\alpha^2\rangle &= \int_{\mathbb{R}^3} \hat{D}_{\alpha\alpha}(\boldsymbol{k}, t)d\boldsymbol{k} \\ &\simeq C(t)\ell^{-5}(t)\int_{\mathbb{R}^3} h_{\alpha\alpha}(\boldsymbol{\zeta})d\boldsymbol{\zeta}. \end{aligned} \tag{17}$$

Because $\boldsymbol{\zeta}$ is time independent, we find that

$$\langle\xi_\alpha^2\rangle\ell^5 \simeq \text{const.} \times C(t). \tag{18}$$

On the basis of Eqs. (6) and (16), the integral length scale of the error field in the x_1 direction, $L_1(\xi_\alpha)$, results in

$$\begin{aligned} L_1(\xi_\alpha) &= \pi\frac{\int_{\mathbb{R}^2} \hat{D}_{\alpha\alpha}(0, k_2, k_3, t)dk_2dk_3}{\int_{\mathbb{R}^3} \hat{D}_{\alpha\alpha}(\boldsymbol{k}, t)d\boldsymbol{k}}, \\ &\simeq \pi\frac{C\ell^{-4}\int_{\mathbb{R}^2} h_{\alpha\alpha}(0, \zeta_2, \zeta_3)d\zeta_2d\zeta_3}{C\ell^{-5}\int_{\mathbb{R}^3} h_{\alpha\alpha}(\boldsymbol{\zeta})d\boldsymbol{\zeta}} \\ &\simeq \text{const.} \times \ell(t). \end{aligned} \tag{19}$$

Similarly, we obtain $L_m(\xi_\alpha) \simeq \text{const.} \times \ell(t)$ for $m = 2$, and 3. Therefore, we denote $L_\alpha(\xi_\alpha)$ as $L^\xi(t)$, irrespective of α. Substituting Eq. (16) into Eq. (5), and using Eqs. (18) and (19), we find that

$$\frac{E_\delta(k,t)}{\langle|\boldsymbol{\xi}|^2\rangle L^\xi} \simeq \text{time independent} \tag{20}$$

at the large scales. Equation (18) reduces to $\langle|\boldsymbol{\xi}|^2\rangle(L^\xi)^5 \simeq \text{const.} \times C(t)$: this result can be obtained by using a dimensional analysis similar to the analysis of Ref. 2 for a certain type of isotropic passive scalar field in 3D incompressible homogeneous turbulence in which the scalar spectrum is proportional to k^4 at $k \to 0$.

The vector potential of an incompressible velocity field plays an important role in the dynamical behavior of Loitsyansky's integral[20] for Batchelor turbulence in which the energy spectrum $E(k)$ takes a form that $E(k) = C_4k^4 + o(k^4)$ at $k \to 0$. The integral is equivalent to C_4.

2.4 Nonlinear error energy interactions

Using a sharp spectral cutoff filter, we can decompose a field $g(\boldsymbol{x})$ into two contributions, a grid scale (GS) contribution $\overline{g}(\boldsymbol{x},k_c)$ and a sub-grid scale (SGS) contribution $g'(\boldsymbol{x},k_c)$, where k_c is the cutoff wavenumber. The GS contribution $\overline{g}(\boldsymbol{x},k_c)$ is defined as

$$\overline{g}(\boldsymbol{x},k_c) = \frac{1}{(2\pi)^3}\int_{\mathbb{R}^3} H(\boldsymbol{x}-\boldsymbol{x}')g(\boldsymbol{x}')d\boldsymbol{x}', \tag{21}$$

$$\hat{H}(\boldsymbol{k}) = \begin{cases} 1 & \text{for} \quad k < k_c \\ 0 & \text{for} \quad k \geq k_c \end{cases}, \tag{22}$$

while the SGS contribution $g'(\boldsymbol{x},k_c)$ is given by $g'(\boldsymbol{x},k_c) = g(\boldsymbol{x}) - \overline{g}(\boldsymbol{x},k_c)$. Note that $\langle\overline{g}(\boldsymbol{x},k_c)g'(\boldsymbol{x},k_c)\rangle = 0$.

Application of this filter to Eq. (2) results in

$$\frac{1}{2}\partial_t\langle|\overline{\boldsymbol{\xi}}|^2\rangle = \mathcal{P}^G(k_c,t) + \mathcal{P}^S(k_c,t) - \nu\langle\partial_j\overline{\xi}_i\partial_j\overline{\xi}_i\rangle, \tag{23}$$

where

$$\mathcal{P}^G(k_c,t) = \langle(\partial_j\overline{\xi}_i)(\overline{\xi}_j\overline{u}_i)\rangle, \tag{24}$$

$$\mathcal{P}^S(k_c,t) = \langle(\partial_j\overline{\xi}_i)(\overline{\xi_j u_i} - \overline{\xi}_j\overline{u}_i)\rangle + \langle(\partial_j\overline{\xi}_i)(\overline{u_j\xi_i} - \overline{u}_j\overline{\xi}_i)\rangle + \langle(\partial_j\overline{\xi}_i)(\overline{\xi_j\xi_i} - \overline{\xi}_j\overline{\xi}_i)\rangle. \tag{25}$$

Here, we used $\nabla\cdot\overline{\boldsymbol{u}} = 0$ and $\nabla\cdot\overline{\boldsymbol{\xi}} = 0$. The two types of nonlinear terms, $\mathcal{P}^G(k_c,t)$ and $\mathcal{P}^S(k_c,t)$, produce the GS error energy $(1/2)\partial_t\langle|\overline{\boldsymbol{\xi}}|^2\rangle$. The term $\mathcal{P}^G(k_c)$ indicates the error energy production arising from GS interactions of $\overline{u}_i$ and $\overline{\xi}_i$, while $\mathcal{P}^S(k_c)$ indicates the error energy production due to the nonlinear interactions of the GS and SGS contributions, $\overline{g}$ and g', where $g = u_i$ or ξ_i.

The decomposition of $\langle(\partial_j\overline{\xi}_i)\overline{\xi_j u_i} + (\partial_j\overline{\xi}_i)\overline{u_j\xi_i} + (\partial_j\overline{\xi}_i)\overline{\xi_j\xi_i}\rangle$ into $\mathcal{P}^G(k_c)$ and $\mathcal{P}^S(k_c)$ is uniquely determined. The expressions of each nonlinear term cannot be uniquely determined. The term $(\partial_j\overline{\xi}_i)\overline{\xi_j u_i}$ can be expressed in other forms, by the use of $u_i^{(1)}$. For example, we can rewrite $(\partial_j\overline{\xi}_i)\overline{\xi_j u_i}$ as $(\partial_j\overline{\xi}_i)\overline{\xi_j u_i} = (\partial_j\overline{\xi}_i)\left(\overline{\xi_j u_i^{(1)}} - \overline{\xi_j\xi_i}\right)$. Accordingly, we do not mention the role of each individual term of $\mathcal{P}^S(k_c)$.

3. Direct Numerical Simulation

3.1 Method and parameters

We performed DNS of two incompressible turbulent flows obeying Eq. (1) with the incompressibility conditions in a $(2\pi)^3$ periodic box, using a Fourier spectral method and a fourth order Runge-Kutta method. The aliasing errors are removed by a phase shift method and a sharp spectral cutoff filter. The Fourier modes satisfying $k < \sqrt{2}N^{1/3}/3$ are retained, where N is the number of grid points and $N = 512^3$. As the force $\boldsymbol{F}$, we employ a negative viscosity only in the low wavenumber range of $k < 2.5$ such that $\langle|\boldsymbol{u}|^2\rangle$ remains unity. The kinematic viscosity ν is 3.2×10^{-4}, and the time increment is 1.0×10^{-3}. Here and in the following, $\langle\cdot\rangle$ denotes the spatial average. The initial time instant t_0 is set to zero.

The initial field $\boldsymbol{u}(\boldsymbol{x}, 0)$ is a statistically quasi-stationary fully-developed turbulent flow obtained by a preliminary DNS using the same method. The Taylor microscale Reynolds number is $R_\lambda = 243$ and $k_{\max}\eta \approx 1$, where R_λ is defined as $R_\lambda = u'\lambda/\nu$, $\lambda = (15\nu u'^2/\langle\epsilon\rangle)^{1/2}$, $u' = \sqrt{\langle|\boldsymbol{u}|^2\rangle/3}(= 1/\sqrt{3})$, $k_{\max}$ is the maximum wavenumber, and η is the Kolmogorov micro-length scale defined by $(\nu^3/\langle\epsilon\rangle)^{1/4}$. The initial field $\boldsymbol{u}^{(1)}(\boldsymbol{x}, 0)$ is slightly different from $\boldsymbol{u}(\boldsymbol{x}, 0)$. The difference exists only in the Fourier modes in a high wavenumber range, $k \geq k_i$, where we set $k_i = 0.985k_{\max}$. The field $\hat{\boldsymbol{u}}^{(1)}(\boldsymbol{k}, 0)$ in $k \geq k_i$ is randomized while keeping the energy spectrum of $\boldsymbol{u}$ and satisfying the solenoidal condition. The initial total error energy is 3.1×10^{-5}.

The DNS was run up to $t \approx 2.5T$, where T is the initial large-eddy turnover time defined as $T = L^u/u'$, and $L^u = (1/3)\{L_1(u_1) + L_2(u_2) + L_3(u_3)\}$ at $t = 0$. The two flows are statistically nearly identical. The spectrum $E^{(0)}(k, t)$ remains almost unchanged and excellently agrees with $E^{(1)}(k, t)$. We confirmed that $L_1(\xi_1) \approx L_2(\xi_2) \approx L_3(\xi_3)$. Therefore, we define L^ξ as

$$L^\xi = \frac{L_1(\xi_1) + L_2(\xi_2) + L_3(\xi_3)}{3}. \tag{26}$$

For brevity, we omit figures presenting $E^{(0)}(k, t)$ and $E^{(1)}(k, t)$ at different time instants and the time development of $L_\alpha(\xi_\alpha)$ $(\alpha = 1, 2, 3)$.

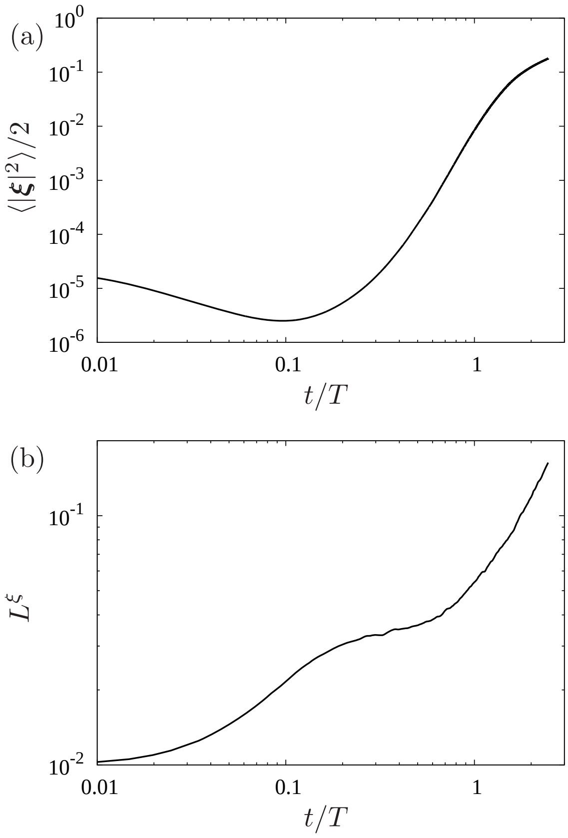

Fig. 1. Evolution of (a) the error energy $(1/2)\langle|\boldsymbol{\xi}^2|\rangle$ and (b) the integral length scale L^ξ.

3.2 Numerical results

Figure 1(a) shows that the error energy grows rapidly for $t/T \gtrsim 0.1$. It can be seen in Fig. 1(b) that the length scale L^ξ increases monotonically with time. Figure 2 shows the error energy spectra $E_\delta(k,t)$ at different time instants. We can see that $E_\delta(k)$ is approximately proportional to k^4 in a low wavenumber range for $0.25 \lesssim t/T \lesssim 2$, i.e., $\tau \lesssim t/T \lesssim 8\tau$, where $\tau \approx 0.25$. The growth of $E_\delta(k)$ with $E_\delta(k) \propto k^4$ is in accordance with the simulation based on the test-field model,[5)] numerical calculations using the EDQNM model,[6)] and the large-eddy simulation results.[7)] Yamazaki *et al.*[21)] examined the influence of the DNS resolutions on incompressible turbulence in a periodic box. The spectrum of the difference field between turbulent flows with $k_{\max}\eta \approx 1$ and $k_{\max}\eta \approx 2$ increases with k as approximately k^4 for a low wavenumber range.

Figure 3 shows the kL^ξ-dependence of the normalized error energy spectra $E_\delta(k)/(\langle|\boldsymbol{\xi}|^2\rangle L^\xi)$. The k^4-like spectra are observed for $kL^\xi \lesssim 0.5$. We can observe good collapse of the normalized spectra for $0.5 \lesssim t/T \lesssim 1.5$, i.e., $2\tau \lesssim t/T \lesssim 6\tau$. This collapse shows that the error growth is well characterized by $\langle|\boldsymbol{\xi}|^2\rangle$ and L^ξ at the large scales of the error

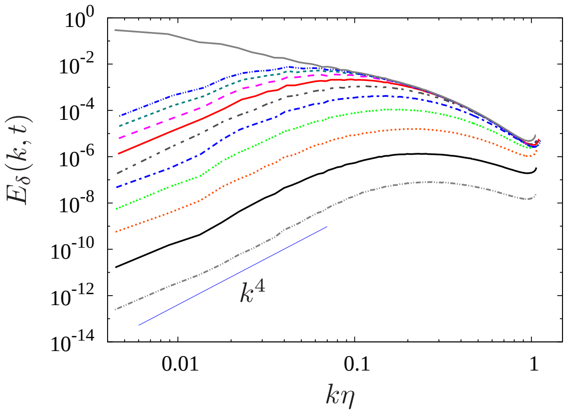

Fig. 2. (Color online) The error energy spectra $E_\delta(k,t)$ versus $k\eta$ at different time instants $t/T = n\tau$ ($n = 1, \cdots, 10$), where $\tau \approx 0.25$. The spectra are plotted from bottom to top starting with $E_\delta(k,\tau)$. The solid gray line denotes $2E^{(0)}(k)$ at $t/T = 0$.

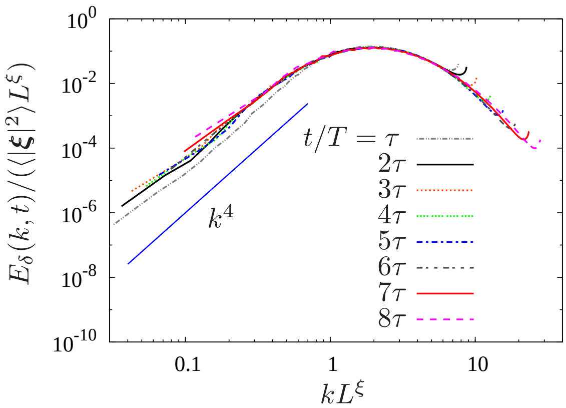

Fig. 3. (Color online) Normalized error energy spectra $E_\delta(k,t)/(\langle|\boldsymbol{\xi}|^2\rangle L^\xi)$ versus kL^ξ at $t/T = n\tau$, where $n = 1, \cdots, 8$.

field including the scales in the error energy containing range. This is in accordance with Eq. (20), which was theoretically obtained on the basis of both a self-similarity assumption of the large-scale error evolution and the large-scale properties of the error field.

In the DNS we consider here, $L^\xi \ll L^u$ and L^u is comparable to the box size. Therefore, the DNS does not resolve the velocity field at $\boldsymbol{k} \to \boldsymbol{0}$ in the sense that $E^{(0)}(k,t)$ does not take a form that $E^{(0)}(k,t) \propto k^b$ at $kL^u \ll 1$ ($1 \le b \le 4$). We thus speculate that the contributions of the unresolved $\hat{\boldsymbol{u}}(\boldsymbol{k})$ to the nonlinear convection terms in Eq. (9) are negligible here. Kida and Ohkitani[8] found the growth of $\Lambda'_2(t)$ in the form that $E_\delta(k,t) \approx \Lambda'_2(t)k^2$ for a low wavenumber range, using DNS in a periodic box. Note that their initial error energy spectrum has its maximum in the low wavenumber range. We discussed the invariance of Λ_2 in the form that

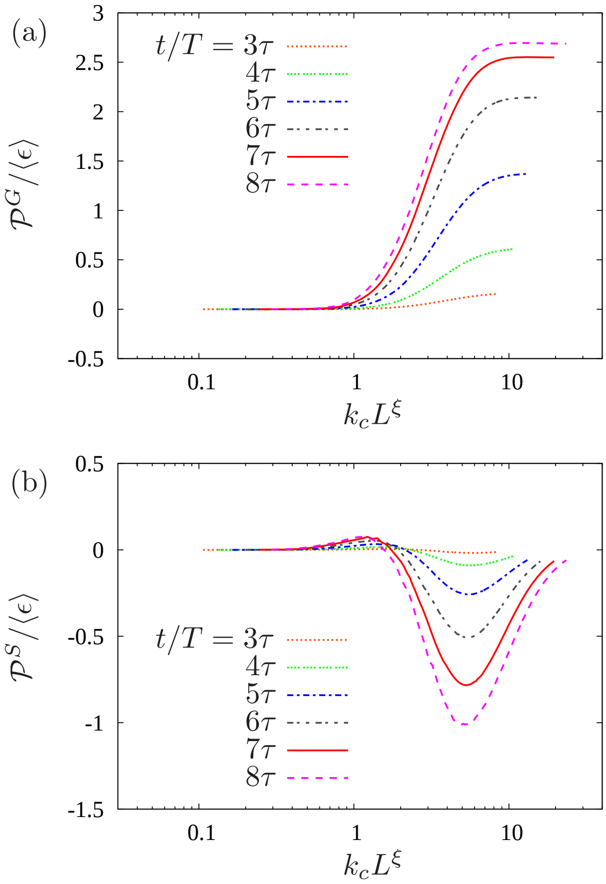

Fig. 4. (Color online) The $k_c L^\xi$-dependence of (a) $\mathcal{P}^G(k_c)/\langle\epsilon\rangle$ and (b) $\mathcal{P}^S(k_c)/\langle\epsilon\rangle$ at $t/T = n\tau$ ($n = 3, \cdots, 8$).

$E_\delta(k, \tilde{t}_0) = \Lambda_2 k^2 + o(k^2)$ at the end of Sec. 2.2. The invariance or the form can break if the large-scale motion is not well resolved owing to the smallness of the computational domain.

To obtain a deeper insight of the nonlinear dynamics in the error growth, we examine two types of scale-dependent error energy production, $\mathcal{P}^G(k_c, t)$ and $\mathcal{P}^S(k_c, t)$, which are defined by Eqs. (24) and (25), respectively. Figures 4(a) and 4(b) show the kL^ξ-dependence of $\mathcal{P}^G(k_c, t)/\langle\epsilon\rangle$ and $\mathcal{P}^S(k_c, t)/\langle\epsilon\rangle$ as functions of $k_c\eta$ at different time instants, respectively, where $\langle\epsilon\rangle$ is quasi-stationary and is the mean kinetic energy dissipation rate of the field $\boldsymbol{u}^{(0)}$. In Fig. 4(a), we can see that $\mathcal{P}^G(k_c, t) > 0$ irrespective of $k_c L^\xi$ and t. This positive production implies that the GS interactions increase the GS error energy $(1/2)\langle|\overline{\boldsymbol{\xi}}|^2\rangle$. The production $\mathcal{P}^G(k_c)$ monotonically increases with k_c. The increment of $\mathcal{P}^G(k_c)$ corresponds to the production of the error energy spectrum $E_\delta(k_c)$. Figure 4(a) shows that the GS interactions actively produce $E_\delta(k_c)$ in the range $2 \lesssim k_c L^\xi \lesssim 5$. In Fig. 4(b), we can see that for $k_c L^\xi \lesssim 2$, $\mathcal{P}^S(k_c) > 0$. This positive $\mathcal{P}^S(k_c)$ means that the GS error energy is produced due to the interactions between the GS and SGS contributions of $\boldsymbol{u}$ and $\boldsymbol{\xi}$. Figure 5 shows that $\mathcal{P}^S(k_c)$ is much larger

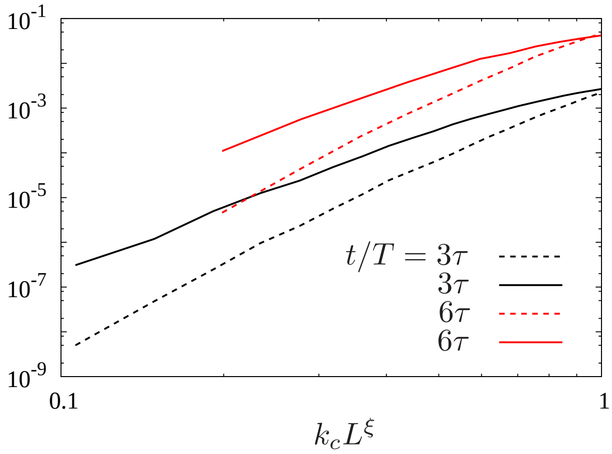

Fig. 5. (Color online) A replot of $\mathcal{P}^S(k_c)/\langle\epsilon\rangle$ and $\mathcal{P}^G(k_c)/\langle\epsilon\rangle$ at $t/T = 3\tau$ and 6τ. The solid and dashed lines denote $\mathcal{P}^S(k_c)/\langle\epsilon\rangle$ and $\mathcal{P}^G(k_c)/\langle\epsilon\rangle$, respectively.

than $\mathcal{P}^G(k_c)$ in $k_c L^\xi \lesssim 0.5$ where the k^4-like error spectra are observed in Fig. 3. Therefore, $\mathcal{P}^S(k_c)$ plays a significant role in the growth of the k^4-like error energy spectrum, which is in accordance with predictions by closure theories.[5,6)] The production $\mathcal{P}^S(k_c, t)$ has a minimum near $k_c L^\xi \approx 5$, irrespective of t. The minimum value is negative and becomes smaller with increasing time, which means that the depletion of the GS error energy due to the interactions between the GS and SGS contributions becomes stronger, as time progresses.

4. Conclusions

We studied the error growth in 3D incompressible homogeneous turbulence. We argued that the error energy spectrum $E_\delta(k, t)$ can grow with time while keeping the form that $E_\delta(k, t) \propto k^4$ at $k \to 0$. It was shown that the growth is well characterized by the error energy $(1/2)\langle|\boldsymbol{\xi}|^2\rangle$ and an integral length scale of the error field L^ξ by the theoretical analysis based on a self-similarity assumption for the error field evolution at the large scales including the scales of the error energy containing range. We carried out DNS of two incompressible turbulent flows in a periodic box at $R_\lambda = 243$. These flows are statistically nearly identical and quasi-stationary. The difference between these velocity fields in $\boldsymbol{k}$ space is initially only in the high wavenumber range. The DNS showed that the normalized spectra $E_\delta(k, t)/(\langle|\boldsymbol{\xi}|^2\rangle L^\xi)$ well collapse in a certain time period, which implies that the characterization of $E_\delta(k, t)$ by both $(1/2)\langle|\boldsymbol{\xi}|^2\rangle$ and L^ξ is appropriate. The spectrum $E_\delta(k, t)$ approximately obeys k^4 in the low wavenumber range, $kL^\xi \lesssim 0.5$. These DNS results suggest that large-scale error field properties play significant roles in the error growth. In addition, the scale-dependent nonlinear error energy production was discussed. A spectral cutoff filter splits the velocity and error fields into two contributions, the GS and SGS contributions. The GS contributions consist only of the Fourier modes of the velocity and error fields satisfying $k < k_c$, while the SGS contributions consist of Fourier modes of the velocity and error fields satisfying $k \geq k_c$. It was shown that the k^4 form of $E_\delta(k)$ is mainly due to the interactions of the GS and SGS contributions. The error energy is produced mainly by the nonlinear interactions of only the GS contributions. These interactions are active in $2 \lesssim k_c L^\xi \lesssim 5$.

The laws governing the time evolutions of $\langle|\boldsymbol{\xi}|^2\rangle$ and L^ξ remain issues. The Reynolds number of the flows obtained by the DNS is not sufficiently high. A DNS study of these laws will require much higher computational cost. A Lagrangian closure theory without ad hoc parameters[22] could be useful.

Acknowledgment

The computations were carried out on the FX1 and FX100 systems at the Information Technology Center of Nagoya University. This work was supported by Grant-in-Aids for Scientific Research (S) JP16H06339 and (C) JP25390149 from the Japan Society for the Promotion of Science.

Appendix: Derivation of Eq. (15)

We define the zeroth order term in k of $\hat{A}_{\alpha\alpha}(\boldsymbol{k}, t)/C(t)$ at $\boldsymbol{k} \to \boldsymbol{0}$ by $\Phi_{\alpha\alpha}(\tilde{\boldsymbol{k}})$: $\Phi_{\alpha\alpha}(\tilde{\boldsymbol{k}}) = P_{i\alpha}P_{j\alpha}\tilde{M}_{ij} = (\delta_{i\alpha} - \tilde{k}_i\tilde{k}_\alpha)(\delta_{j\alpha} - \tilde{k}_j\tilde{k}_\alpha)\tilde{M}_{ij}$, where $\tilde{\boldsymbol{k}} = \boldsymbol{k}/k$ and $|\tilde{\boldsymbol{k}}| = 1$. In the self-similar state, $\Phi_{\alpha\alpha}(\tilde{\boldsymbol{k}})$ is time-independent. Let us consider the domain where $0 < \tilde{k}_1 < 1$ and $\tilde{k}_3 = 0$. We obtain $\tilde{k}_1 = 1/\sqrt{1+\sigma}$ and $\tilde{k}_2 = \sigma/\sqrt{1+\sigma}$, where $\sigma = \tilde{k}_2/\tilde{k}_1 = k_2/k_1$. Expanding $\Phi_{\alpha\alpha}(\tilde{\boldsymbol{k}})$ in the powers of σ for $|\sigma| \ll 1$ at $\tilde{k}_3 = 0$, we have

$$\Phi_{\alpha\alpha}(\tilde{k}_1, \tilde{k}_2, 0) = \sum_{m=0}^{\infty} \Xi_m \sigma^m, \tag{A·1}$$

where Ξ_m is a constant independent of t and $\tilde{\boldsymbol{k}}$. Therefore, $\Phi_{\alpha\alpha}(\tilde{k}_1, \tilde{k}_2, 0)$ is a function of only σ. Equation (14) gives

$$\Phi_{\alpha\alpha}(\tilde{k}_1, \tilde{k}_2, 0) = f^0_{\alpha\alpha}(\tilde{\zeta}_1, \tilde{\zeta}_2, 0) \tag{A·2}$$

at $\boldsymbol{k} \to \boldsymbol{0}$ implying $\boldsymbol{\zeta} \to \boldsymbol{0}$, where $f^0_{\alpha\alpha}(\tilde{\boldsymbol{\zeta}})$ is the zeroth order term in $|\boldsymbol{\zeta}|$ of $f_{\alpha\alpha}(\boldsymbol{\zeta})$ and $\tilde{\boldsymbol{\zeta}} = \boldsymbol{\zeta}/|\boldsymbol{\zeta}|$. Equations (A·1) and (A·2) imply that $f^0_{\alpha\alpha}(\tilde{\zeta}_1, \tilde{\zeta}_2, 0)$ is a function of only $\lambda' = \tilde{\zeta}_2/\tilde{\zeta}_1$ for small σ, because the right-hand side is a function of only $\tilde{\zeta}_1$ and $\tilde{\zeta}_2$, while the left-hand side is a function of only σ. It is to be noted that $\sigma = \gamma\lambda'$ where $\gamma = \ell_1/\ell_2$. Hereafter we write $\Phi_{\alpha\alpha}(\tilde{k}_1, \tilde{k}_2, 0)$ and $f^0_{\alpha\alpha}(\tilde{\zeta}_1, \tilde{\zeta}_2, 0)$ as $\Phi_{\alpha\alpha}(\gamma\lambda')$ and $f^0_{\alpha\alpha}(\lambda')$. Because $f^0_{\alpha\alpha}(\tilde{\boldsymbol{\zeta}})$ is time independent for any $\tilde{\boldsymbol{\zeta}}$, we find that $\left[(d^n/d\lambda'^n)f^0_{\alpha\alpha}(\lambda')\right]_{\lambda'=0}$ is time independent for a positive integer n.

Here, we can take $n = 2$ because $\Xi_2 \neq 0$ in general. Using Eq. (A·2), we find that

$$\left[\frac{\partial^n}{\partial \lambda'^n}\Phi_{\alpha\alpha}(\gamma\lambda')\right]_{\lambda'=0} = n!\Xi_n\gamma^n = \text{time independent}, \tag{A·3}$$

which implies that $\gamma(= \ell_1/\ell_2)$ is constant. In the same way, we find that ℓ_1/ℓ_3 is also constant. Therefore, we obtain Eq. (15).

References

1) E. N. Lorenz, Tellus **21**, 289 (1969).

2) M. Lesieur, *Turbulence in Fluids* (Kluwer Academic Publishers, Dordrecht, 1993) 2nd ed.

3) Y. Zhou, C. E. Leith, J. R. Herring, and Y. Kimura, Mech. Res. Commun. **39**, 15 (2012).

4) J. R. Herring, J. J. Riley, G. S. Patterson, and R. H. Kraichnan, J. Atmos. Sci. **30**, 997 (1973).

5) C. E. Leith and R. H. Kraichnan, J. Atmos. Sci. **29**, 1041 (1972).

6) O. Métais and M. Lesieur, J. Atmos. Sci. **43**, 857 (1986).

7) J.-P. Chollet and O. Metais, Eur. J. Mech., B/Fluids **8**, 523 (1989).

8) S. Kida and K. Ohkitani, Phys. Fluids A **4**, 1018 (1992).

9) A. Berera and R. D. J. G. Ho, Phys. Rev. Lett. **120**, 024101 (2018).

10) G. Boffetta and S. Musacchio, Phys. Rev. Lett. **119**, 054102 (2017).

11) P. Mohan, N. Fitzsimmons, and R. D. Moser, Phys. Rev. Fluids **2**, 114606 (2017).

12) T. Ishida, P. A. Davidson, and Y. Kaneda, J. Fluid Mech. **564**, 455 (2006).

13) N. Okamoto, P. A. Davidson, and Y. Kaneda, J. Fluid Mech. **651**, 295 (2010).

14) P. A. Davidson, N. Okamoto, and Y. Kaneda, J. Fluid Mech. **706**, 150 (2012).

15) K. Yoshimatsu and Y. Kaneda, Phys. Rev. Fluids **4**, 024611 (2019).

16) G. K. Batchelor, *The Theory of Homogeneous Turbulence* (Cambridge University Press, Cambridge, U.K., 1953).

17) G. K. Batchelor and I. Proudman, Philos. Trans. R. Soc. London A **248**, 369 (1956).

18) K. Yoshimatsu and Y. Kaneda, Phys. Rev. Fluids **3**, 104601 (2018).

19) P. G. Saffman, J. Fluid Mech. **27**, 581 (1967).

20) P. A. Davidson, J. Fluid Mech. **632**, 329 (2009).

21) Y. Yamazaki, T. Ishihara, and Y. Kaneda, J. Phys. Soc. Jpn. **71**, 777 (2002).

22) Y. Kaneda, Fluid Dyn. Res. **39**, 526 (2007).